Next-Generation Sequencing in Diffuse Large B-Cell Lymphoma Highlights Molecular Divergence and Therapeutic Opportunities: a LYSA Study

Sydney Dubois, Pierre-Julien Viailly, Sylvain Mareschal, Elodie Bohers, Philippe Bertrand, Philippe Ruminy, Catherine Maingonnat, Jean-Philippe Jais, Pauline Peyrouze, Martin Figeac, et al.

Next Generation Sequencing in Diffuse Large B Cell Lymphoma Highlights Molecular Divergence and Therapeutic Opportunities: a LYSA Study

Sydney Dubois[1], Pierre-Julien Viailly[1,2], Sylvain Mareschal[1], Elodie Bohers[1], Philippe Bertrand[1], Philippe Ruminy[1], Catherine Maingonnat[1], Jean-Philippe Jais[3], Pauline Peyrouze[4], Martin Figeac[4], Thierry J Molina[5], Fabienne Desmots[6], Thierry Fest[6], Corinne Haioun[7], Thierry Lamy[6], Christiane Copie-Bergman[8], Josette Brière[9,10], Tony Petrella[11], Danielle Canioni[12], Bettina Fabiani[13], Bertrand Coiffier[14], Richard Delarue[15], Frédéric Peyrade[16], André Bosly[17], Marc André[17], Nicolas Ketterer[18], Gilles Salles[14], Hervé Tilly[1], Karen Leroy[19], Fabrice Jardin[1]

1 Inserm U918, Centre Henri Becquerel, Université de Rouen, IRIB, Rouen, France
2 LITIS EA 4108, Normandie Université, Rouen, France
3 Inserm UMRS 872, AP-HP Hôpital Necker, Paris, France
4 Université de Lille 2, Lille, France
5 Pathology, AP-HP, Hôpital Necker, EA 7324, Université Paris Descartes, France
6 Inserm U917, CHU Pontchaillou, Rennes, France
7 Unité Hémopathies Lymphoïdes, AP-HP Hôpital Henri Mondor, Créteil, France
8 IMRB – Inserm U955, AP-HP Hôpital Henri Mondor, Créteil, France
9 Inserm U728, Université Paris Diderot, Sorbonne Paris Cité
10 Department of Pathology, AP-HP Hôpital Saint-Louis, Paris, France
11 Department of Pathology, Hôpital Maisonneuve-Rosemont, Montréal (QC), H1T2M4, Canada
12 Laboratoire de Pathologie, AP-HP Hôpital Necker, Paris, France
13 Laboratoire de Pathologie, AP-HP Hôpital Saint Antoine, Paris, France
14 CNRS UMR5239, Hospices Civils de Lyon, Lyon, France
15 Department of Hematology, AP-HP Hôpital Necker, Paris, France
16 Department of Hematology, Lacassagne Center, Nice, France
17 CHU Dinant Godinne, UcL Namur, Yvoir, Belgium
18 Department of Oncology, Lausanne Hospital, Lausanne, Switzerland
19 Inserm U955 Team 09, AP-HP Hôpital Henri Mondor, Créteil, France

Running Title: Targeted NGS details DLBCL divergence and actionable targets

Corresponding author: Fabrice Jardin
Address: 1 rue d'Amiens, Centre Henri Becquerel, Rouen, France
Email: fabrice.jardin@chb.unicancer.fr
Phone: +33 (0)232082465
Fax: +33 (0)232082455

Keywords: Diffuse Large B Cell Lymphoma, Primary Mediastinal B-cell Lymphoma, Next Generation Sequencing

Declaration of Interests: The authors disclose no potential conflicts of interest.

Total word count: 3866, Abstract word count: 247, Number of figures and tables: 6

Translational Relevance

This is the first Next Generation Sequencing (NGS) study of such a large, prospective cohort using a targeted gene panel, the Lymphopanel, focusing on genes identified as important for lymphomagenesis or whose potential has been pinpointed in Whole Exome Sequencing studies. Particular attention has been paid to the inclusion of actionable targets in the Lymphopanel, highlighting potential candidate patients for novel personalized therapies. This study further details subtype-enriched gene and pathway mutations in order to optimize DLBCL treatment, and highlights several novel, frequent, and actionable mutations, notably in PMBL. In addition, Lymphopanel NGS has enabled the detection of novel clinical and prognostic correlations, potentially impacting treatment decisions. As benchtop sequencers become increasingly available in academic research and routine clinical settings, our study demonstrates the feasibility and impact of NGS with a consensus gene panel in DLBCL patient management, contributing essential information to today's precision therapy era treatment decisions.

Abstract

Purpose: Next Generation Sequencing (NGS) has detailed the genomic characterization of Diffuse Large B Cell Lymphoma (DLBCL) by identifying recurrent somatic mutations. We set out to design a clinically feasible NGS panel focusing on genes whose mutations hold potential therapeutic impact. Furthermore, for the first time, we evaluated the prognostic value of these mutations in prospective clinical trials.

Experimental Design: A Lymphopanel was designed to identify mutations in 34 genes, selected according to literature data and a whole exome sequencing study of relapsed/refractory DLBCL patients. The tumor DNA of 215 patients with CD20+ *de novo* DLBCL in the prospective, multicenter and randomized LNH-03B LYSA clinical trials was sequenced to deep, uniform coverage with the Lymphopanel. Cell of origin molecular classification was obtained through gene expression profiling with HGU133+2.0 Affymetrix GeneChip arrays.

Results: The Lymphopanel was informative for 96% of patients. A clear depiction of DLBCL subtype molecular heterogeneity was uncovered with the Lymphopanel, confirming that Activated B Cell-like (ABC), Germinal Center B-cell like (GCB) and Primary Mediastinal B-cell Lymphoma (PMBL) are frequently affected by mutations in NFkB, epigenetic, and JAK-STAT pathways respectively. Novel truncating immunity pathway, *ITPKB*, *MFHAS1* and *XPO1* mutations were identified as highly enriched in PMBL. Notably, *TNFAIP3* and *GNA13* mutations in ABC patients treated with R-CHOP were associated with significantly less favorable prognoses.

Conclusions: This study demonstrates the contribution of NGS with a consensus gene panel to personalized therapy in DLBCL, highlighting subtypes' molecular heterogeneity and identifying somatic mutations with therapeutic and prognostic impact.

Introduction

Diffuse large B-cell lymphoma (DLBCL) is the most common form of adult lymphoma worldwide, accounting for 30-40% of newly diagnosed Non-Hodgkin Lymphoma (NHL)(1). Gene expression profiling (GEP) has made strides in deciphering the molecular heterogeneity of DLBCL, enabling the entity's subdivision into three main molecular subtypes: Germinal Center B-cell like (GCB), Activated B-Cell like (ABC), and Primary Mediastinal B-cell Lymphoma (PMBL)(2,3). Among other genetic aberrations, the GCB subtype is characterized by t(14;18)(q32;q21) translocations(4) and loss of *PTEN*(5), while the ABC subtype is characterized by t(3;14)(q27;q32) translocations, deletion of the INK4A-ARF locus(6) and *BCL2* amplification(7). PMBL displays strong molecular similarities to classical Hodgkin Lymphoma (cHL), exhibiting frequent amplifications of *JAK2* and deletions of *SOCS1*(8,9). Arising from B cells at distinct stages of differentiation and maturation, these subtypes are also diverse in clinical presentation, response to immunochemotherapy and outcome, with the ABC subtype having the most unfavorable prognosis(2,7). As targeted therapies become increasingly widespread, it is essential to thoroughly characterize each molecular subtype, in order to ensure optimal care for each patient. Unfortunately, the cell of origin (COO) classification of DLBCL still has relatively little influence on clinical practice, as GEP is poorly transposable to routine diagnosis and surrogate immunohistochemical algorithms remain unreliable(10), although recent techniques offer better bench to bedside translation(11,12).

Next generation sequencing (NGS) technologies, enabling high-throughput DNA sequencing, have emerged over the past decade and have provided new insights into the genomic characterization of DLBCL by identifying recurrent single nucleotide variants (SNVs), which can be enriched in a particular subtype(13–22). Although DLBCL is defined by widespread genetic heterogeneity, several of the pinpointed recurrent SNVs warrant special interest as they occur in actionable targets and/or correlate with antitumoral response. Equally of note, despite their probable physiopathological relevance, neither the prognostic value of these mutations nor their potential to predict resistance to conventional B-cell lymphoma immunochemotherapy treatment has been properly evaluated in prospective clinical trials. Furthermore, mutation feature analyses have identified activation-induced cytidine deaminase (AID)-driven somatic hypermutation (SHM) as a mechanism mediating the development of

some of these recurrent SNVs, rendering the task of distinguishing driver from passenger mutations even more challenging(23).

To more feasibly identify molecular subtypes and reach the goal of precision therapy in DLBCL, a limited and clinically relevant panel of target genes must be designed, with efforts made to thoroughly describe the SNVs they harbor. Furthermore, compact sequencers readily available in academic laboratories must be used in order to generalize this practice and apply it to routine clinical disease management. With this idea in mind, we developed a Lymphopanel NGS assay, designed to identify mutations in 34 genes important for lymphomagenesis based on a literature review of WES studies in DLBCL(13,14,20,24) as well as a WES study of relapsed/refractory DLBCL cases(25). In the current study, we sequenced 215 patients with *de novo* DLBCL enrolled in the prospective, multicenter and randomized LYSA LNH-03B trials, using the Lymphopanel. Our intent was to determine whether the Lymphopanel was informative enough to identify targetable SNVs and/or pathway mutations that might alter treatment decisions, highlight subtype-specific mutational profiles, distinguish genes impacted by AID, and potentially foretell clinical outcome.

Materials and Methods

Patients

215 adult patients with de novo CD20+ DLBCL enrolled in the prospective, multicenter and randomized LNH-03B LYSA trials with available frozen tumor samples, centralized histopathological review and adequate DNA/RNA quality were selected. The LNH03-B LYSA trials were initiated in 2003 and included 1704 patients overall in six distinct clinical trials (Supplementary Methods). COO molecular classification was obtained with HGU133+2.0 Affymetrix GeneChip arrays (Affymetrix), grouping patients into ABC, GCB, PMBL and “other”, also referred to as unclassified (detailed in Supplementary Methods). Clinical features of the patients are indicated in Table S1. The study was performed with approval of an institutional review board and written informed consent was obtained from all participants at the time of enrollment.

NGS experiments and data analysis

The Lymphopanel was designed to identify mutations in 34 genes important for lymphomagenesis, based on literature data (Table S2)(24) and WES of relapsed/refractory

DLBCL sequencing(25). The design covers 87 703 bases using 872 amplicons. Genes were grouped into 8 specific pathways: Immunity (*CIITA*, *B2M*, *TNFRSF14* and *CD58*), NOTCH (*NOTCH1* and *NOTCH2*), Apoptosis/Cell cycle (*MFHAS1*, *XPO1*, *MYC*, *CDKN2A*/*B*, *FOXO1*, *TP53*, *GNA13* and *BCL2*), NFkB (*TNFAIP3*, *MYD88*, *PIM1*, *CARD11*, *IRF4* and *PRDM1*), Epigenetic Regulation (*EZH2*, *KMT2D*, *EP300*, *MEF2B* and *CREBBP*), MAP Kinase (*BRAF*), JAK-STAT (*SOCS1* and *STAT6*), and BCR (*CD79A*/*B*, *ITPKB*, *TCF3* and *ID3*) (Table S3).

Ion Torrent Personal Genome Machine (PGM) Sequencing and PGM data analysis was performed as previously described(26) and detailed in Supplementary Methods. Variant analysis was performed using an in-house generated bioinformatics pipeline, detailed in Supplementary Methods and Figures S1 and S2. This pipeline ensured excellent filtering of artefacts and polymorphisms, as proven by an independent study of seven non-tumoral samples from DLBCL patients with a mean error rate of non-filtered variants of only 0.7% (Table S4).

Statistical methods

All statistical analyses were performed using R software version 3.1.2(27). Progression-Free survival (PFS) was evaluated from the date of enrolment to the date of disease progression, relapse, re-treatment or death from any cause. Overall survival (OS) was evaluated from the date of enrolment to the date of death from any cause. Multivariate Cox and log-rank tests ("survival" R package version 2.37.7) were used to assess differences in OS and PFS rates calculated by Kaplan-Meir estimates. Ward hierarchical unsupervised clustering ("LPS" R package version 1.0.10) was performed using Jaccard distance. Statistical differences between all other parameters were determined using χ^2, Mann-Whitney or Fisher's exact tests when appropriate. P values or False Discovery Rates (FDR) < 0.05 were considered statistically significant.

Results and Discussion

Lymphopanel Variant Features

Lymphopanel NGS was performed on 215 DLBCL patients (81 ABC, 83 GCB, 33 "other" and 18 PMBL). The median overall sequencing depth was 225x [110x-331x]. An initial 13 965 variants were filtered for quality, SNPs and functional relevance, leading to 1064 (7.6%) variants ultimately validated (Table S5 and Figure S1). The Lymphopanel

informativity was of 96%, with 206 patients (78 GCB, 80 ABC, 30 "other" and 18 PMBL) presenting at least one variant. All genes in the Lymphopanel were informative for at least one patient, with the number of variants per gene ranging from one to 124. Gene mutation frequencies in the total cohort and by subtype are presented in Figure 1.

We subdivided the genes targeted by the Lymphopanel into eight specific pathways (Figure 2, Table S3). As expected, we confirmed that the ABC subtype is dominated by NFkB pathway mutations (45% of total variants), followed by epigenetic regulation pathway mutations (20.2% of total variants) (Figure 2A), whereas the GCB subtype is mostly characterized by mutations in the epigenetic regulation pathway (32.3% of total variants) and the apoptosis/cell cycle pathway (26.3% of total variants) (Figure 2B). Mutations in the JAK-STAT, immunity and apoptosis/cell cycle pathways were prevalent in PMBL (29.1%, 20.9% and 20.9% of total variants respectively) (Figure 2C). Interestingly, PMBL presented a significantly higher number of variants per sample than the other subtypes combined ($p=2.76x10^{-5}$, Figure S3). The "other" subtype showed a fairly hybrid spectrum of pathway mutations (Figure 2D), perhaps suggesting the involvement of the three main subtypes, rather than the existence of a distinct entity.

We sought to assess the impact of AID involvement in the Lymphopanel genes (detailed in Supplementary Methods and Figure S4). Genes with an AID mutation frequency superior to the average of that of the Lymphopanel are presented in Table S6. Previously identified SHM targets in DLBCL among these genes include *MYC*, *PIM1*, *IRF4*, *BCL2*, *SOCS1* and *CIITA*(23). Potentially novel SHM targets include *MFHAS1*, *PRDM1*, *GNA13*, *MYD88*, *ITPKB* and *NOTCH2*. There was no significant difference in AID involvement between DLBCL subtypes.

Lymphopanel NGS identifies mutations with potential treatment impact

The Lymphopanel included genes whose mutations could serve to stratify patients according to treatment options. This includes actionable mutations, currently targeted by precision therapies, highlighted in Figure 1, as well as mutations whose presence might call into question the use of certain targeted therapy options.

Recent results have shown that doubly mutated *MYD88*/*CD79B* patients are significantly more responsive to single therapy Ibrutinib, a BTK inhibitor, highlighting the importance of targeted NGS for DLBCL patients in the clinical setting(28). Furthermore, the presence of *CARD11* and *TNFAIP3* mutations has been shown to lead to decreased activity of both Ibrutinib and Sotrastaurin, a Protein Kinase C inhibitor(29,30). *MYD88* mutations are frequent

in ABC DLBCL, L265P being the most prevalent variant (up to 29% in previous studies)(18). In our cohort, *MYD88* mutations were significantly enriched in ABC patients (28.4%, FDR=$4.7x10^{-3}$), with the L265P mutation present in 21% of ABC patients (Figures 3 and S5A). Of 17 ABC patients with *MYD88* L265P mutations, we found ten (58.8%) with associated *CD79B* mutations, who might respond more favorably to Ibrutinib treatment. *CD79B* mutations were identified in 10.7% of total patients, slightly less than previously reported, but were significantly enriched in ABC DLBCL (24.7%, FDR=$3.2x10^{-5}$), corroborating previous studies(13,31). Of note, two (11.8%) MYD88 L265P mutated ABC patients were *CARD11* mutated and two were *TNFAIP3* mutated, potentially diminishing the effect of Ibrutinib and Sotrastaurin, while six (35.3%) were *PRDM1* mutated (Figure S6).

ABC cells have been shown to be addicted to IRF4 activity (32), responsible for Lenalidomide treatment response. 21 *IRF4* variants were discovered in 7.9% of patients (13.6% of ABC, 4.8% of GCB, 0% of "other" and 11.1% of PMBL) (Figure 1). Although the impact on expression of these mutations was not analyzed, only one *IRF4* variant was a stop-gain mutation, indicating that expression is most likely at least conserved. Most of the non-synonymous SNVs were clustered around amino acid positions 18 (two S18 variants and two G20 variants) and 99 (four C99R variants, SIFT scores=0) (Figure 4). Interestingly, *IRF4* mutations were almost equally frequent in PMBL and ABC in our cohort. Although IRF4 addiction has not been demonstrated in PMBL, this predilection for *IRF4* mutations, added to the well-known high expression of IRF4 in this subtype, may suggest a potential role for Lenalidomide treatment in this subtype as well, calling for further investigation of these mutations' effects.

Recently, small molecule inhibitors of PIM kinases have been developed and studied in DLBCL. In our cohort, *PIM1* mutations were significantly skewed toward ABC (33.3%, FDR=$3.3x10^{-5}$) in our cohort and represented 20.2% of ABC variants (Figures 2A, 3 and S5A). Of note, truncating *PIM1* variants were predominant in ABC patients (13 of 14 identified). Interestingly, DLBCL sensitivity to PIM kinase inhibitors is not correlated with the level of PIM kinase expression (33), suggesting that even expression-modifying *PIM1* mutations might not necessarily hamper the efficacy of PIM1 inhibitors, although this remains to be verified. In any case, the high frequency of *PIM1* mutations in our cohort seems to justify the pre-screening of PIM kinase inhibitor candidate patients by *PIM1* sequencing, in order to identify those most likely to benefit from this targeted therapy.

The most highly mutated gene in GCB, *BCL2*(34), can notably be targeted by BH3-mimetics. Among our GCB cohort, *BCL2* was the third most frequently mutated gene (24.1%,

FDR=2.5x10^{-5}) (Figures 3 and S5B), with mutations most frequently impacting the amino terminus and between the BH1 and BH3 domains. The BH3 domain was not impacted, indicating that BH3 mimetic activity would not be hampered in these patients (Figure S7).

Targeting epigenetic changes is also being increasingly explored in the realm of tailored therapy, notably among the GCB subtype, justifying the inclusion of genes such as *EZH2*, *CREBBP*, *KMT2D* and *EP300* within the Lymphopanel. In our cohort, 18.1% of GCB patients were *EZH2* mutated, mostly at the Y641 hotspot, and *EZH2* mutations were enriched in GCB (FDR=1.8x10^{-3}), as observed in previous studies, with no *EZH2* mutated ABC patients(13) (Figures 3 and S5B). Interestingly, one PMBL patient presented an EZH2 Y641 mutation, adding to the debate of which DLBCL subtypes might benefit from EZH2 inhibitor treatment(26). *CREBBP* mutations were identified in 31.3% of GCB patients and 6.2% of ABC patients, corroborating previous studies(17), but were also found in 24.2% of "other" and 11.1% of PMBL (Figures 1 and S5). *KMT2D* mutations, evenly distributed throughout the coding sequence, were identified in 40.9% of our cohort, with *KMT2D* being the most frequently mutated gene in all subtypes except PMBL (Figure 1). Of the 124 variants, 78 were truncating mutations, indicating bias toward loss of protein expression.

Mutations of master regulators *TP53* and *MYC* showed no significant difference in subtype distribution in our cohort (Figure 3). *TP53* variants were present in 14.9% of total patients (slightly less than previously reported(13,35)) (Figure 1) and several recurrent variants were identified, including six R248 variants, shown to be loss of function mutants in DLBCL(35). As for *MYC*, we discovered mutations in 6.5% of total patients (4.9% of ABC, 9.6% of GCB, 3% of "other" and 5.6% of PMBL). No mutations were identified at the known hotspots in Burkitt Lymphoma (BL), including S62 and T58.

Finally, although frequent mutations are most enticing for therapeutic potential, rare mutations can also be potentially very effectively actionable. For instance, *BRAF* and *NOTCH1* mutations have been identified as rare but functionally relevant in DLBCL(13). In our cohort, we identified one patient with an activating V600E *BRAF* variant. As for *NOTCH1*, ten patients in our cohort presented mutations (Figure 1). *TCF3* was mutated in three patients, all of whom harbored a pathogenic N551K variant, which has shown altered DNA-binding specificity(36). The negative regulator of TCF3, ID3, was mutated in 4.7% of patients (Figure 1), with most variants affecting the HLH domain (Figure S7), potentially impairing its ability to inactivate TCF3, as shown in BL(36). *ID3* and *TCF3* mutations have recently been shown to be of comparable frequency in BL and DLBCL, highlighting the overlap between these two entities(37).

The Lymphopanel highlights a unique PMBL mutational signature

STAT6 and *SOCS1* mutations were both very significantly enriched in PMBL (FDR=$6.8x10^{-14}$ and FDR=$2.5x10^{-5}$ respectively), with *STAT6* being the most frequently mutated gene in PMBL (72.2%, Figures 3 and S5C). All *STAT6* mutations were non-synonymous SNVs and recurrent variants were frequent among PMBL, including seven N417 variants (Figure S7). *SOCS1* mutations were present in 55.5% of PMBL patients, 30% of them harboring SOCS1 inactivating mutations (Figure S5C). *TNFAIP3* mutations have also been frequently identified in PMBL (up to 36%)(38). We found *TNFAIP3* mutations to be significantly enriched in PMBL (61.1%, FDR=$3.1x10^{-5}$), with all but one *TNFAIP3* mutated PMBL patient harboring truncating mutations (Figures 3 and S5C). The frequent *TNFAIP3* and *SOCS1* mutations in PMBL highlight the similarities between PMBL and cHL(38,39). Furthermore, no *MYD88*, *CD79B* or *CARD11* mutations were observed in PMBL patients (Figure 1), suggesting a PMBL dependence on *TNFAIP3* mutations for the constitutive activation of NFkB. Interestingly, significant *GNA13* mutation enrichment was shown in PMBL rather than GCB in our cohort (50%, FDR=$2.8x10^{-4}$) (Figures 3 and S5), and one third of *GNA13* variants were potentially truncating mutations (Figure 4).

We discovered 46 *B2M* variants in 18.1% of total patients, significantly enriched in PMBL (50%, FDR=$1.2x10^{-3}$) (Figures 1, 3 and S5C). Six of nine *B2M* mutated PMBL patients harbored truncating mutations and the remaining three presented pathogenic non-synonymous SNVs, two of which were a highly recurrent p.M1R variant predicted to affect the start codon (Figure 4). Recently, frequent *B2M* mutations leading to lack of protein expression were identified in cHL(9). Our similar findings in PMBL further highlight the molecular similarities between these two entities. *CD58* variants were also significantly enriched in PMBL (FDR=$1.2x10^{-3}$) (Figures 3 and S5), with five of seven *CD58* mutated PMBL patients exhibiting truncating mutations, potentially leading to a lack of CD58 expression. Importantly, PD-1 blockade has recently shown promise as an effective treatment of relapsed or refractory cHL(40). Escape from T cell immunity via B2M and/or CD58 mutations could potentially affect the activity of PD-1 inhibitors in PMBL and cHL and warrants further investigation. Furthermore, we found 39 *CIITA* variants, enriched in PMBL as well (55.6% of PMBL versus 14.14% of total patients, FDR=$3.1x10^{-5}$) (Figures 1, 3 and S5C). To our knowledge, this is the first study to identify truncating immunity pathway mutations as major in PMBL, although *CIITA*/*PDL1-2* translocations had been shown to impact PMBL survival(41).

ITPKB, *MFHAS1* and *XPO1* mutations were identified as significantly overrepresented in a relapsed/refractory DLBCL patient cohort(25), leading to their inclusion in the Lymphopanel. In our cohort, *ITPKB*, *MFHAS1* and *XPO1* mutations were all identified for the first time as being significantly enriched in PMBL patients (FDR=$1.4x10^{-2}$, FDR=$3.9x10^{-3}$ and FDR=$4.8x10^{-10}$ respectively, Figure 3). The roles of *ITPKB* and *MFHAS1* in lymphomagenesis are not yet fully elucidated. ITPKB regulates B cell survival and function, and ITPKB deficiency leads to B cell antigen presentation unresponsiveness and decreased B cell survival, associated with specific overexpression of proapoptotic Bim protein(42). We found 48 *ITPKB* variants, present in 14% of total patients (Figures 1 and S5). ITPKB mutations were uniformly distributed along the protein sequence, excepting the seemingly conserved catalytic IPK domain, affected by only two non-synonymous SNVs (Figure 4). *MFHAS1* is a potential oncogene with highly conserved leucine-rich tandem repeats, isolated from a minimal common amplified region in malignant fibrous histiocytomas at 8p23.1. *MFHAS1* is also a target gene for chromosomal translocation t(8;14)(p23.1;q21) in B-cell lymphoma cell lines and has been shown to be tumorigenic in nude mice(43). In our cohort, *MFHAS1* variants were identified in 7.9% of total patients, and were distributed homogeneously along the coding sequence, with no recurrent mutations identified (Figure 4). Although the role of these potential oncogenes in lymphomagenesis is still unclear, their high mutation frequency in PMBL especially warrants further investigation.

As for *XPO1*, it encodes CRM1, an exporter of several tumor suppressor proteins (TSPs). Cytoplasmic export of TSPs renders them inactive, indicating that *XPO1* acts as a proto-oncogene. *XPO1* mutations were present in 4.7% of total patients (1.2% of ABC, 1.2% of GCB, 3% of "other" and 38.9% of PMBL) (Figures 1 and S5). The mutation identified is recurrent, with all variants affecting E571 (Figure 4), as previously found in rare CLL cases (<5%)(44). Importantly, Selective Inhibitors of Nuclear Export (SINEs), have been shown to effectively target CRM1 and retain TSPs in the nucleus(45). Given the frequency of XPO1 E571 mutations in PMBL, further investigation concerning their impact on response to SINEs is warranted (Jardin et al, under review).

Identification of gene mutations correlated with clinical characteristics and prognosis

We tested each gene in the Lymphopanel for correlation with clinical characteristics including age, stage, IPI, bone marrow involvement and presence of bulky disease.

CD79B, *KMT2D* and *MYD88* mutations were significantly correlated with age (Figure S8). For *CD79B* and *MYD88* mutations, enriched in ABC, this might be linked to the significantly

higher age of ABC patients ($p=1.01x10^{-7}$ in our cohort)(46). As for *KMT2D* mutations, homogenous among subtypes, this result potentially suggests an accumulation of passenger-type mutations, particularly visible in this long gene (16.6 kb sequenced). *MYD88* mutations were also significantly correlated with higher IPI (FDR=0.04).

On the other hand, PMBL patients were significantly younger ($p=1.21x10^{-8}$) and the large majority of genes whose mutations were significantly enriched in PMBL were also correlated with younger age (Figure S8). In addition, *B2M* and immunity pathway mutations were significantly inversely correlated with Ann Arbor stage ($FDR=3.2x10^{-3}$ and FDR=0.045 respectively), and *B2M* and *STAT6* mutations were significantly inversely correlated with IPI ($FDR=5.5x10^{-4}$ and FDR=0.026 respectively).

As expected, OS and PFS decreased with increasing IPI and ABC patients displayed significantly worse OS and PFS than GCB patients in the R-CHOP treatment group ($p=1.9x10^{-2}$ and $p=6.6x10^{-3}$ respectively) (Figure S9). Of note, PMBL patients in our cohort did not present the favorable prognosis typically associated with this subtype(47), perhaps due to the lack of dedicated treatment.

Prognostic impact was assessed for all Lymphopanel genes and subtypes, among patients treated with R-chemotherapy, separated into an R-CHOP group and an R-ACVBP group. Analyses over all subtypes were performed using multivariate Cox tests, while analyses of each subtype individually were performed using log-rank tests. In both cases, independent corrections of p-values were performed for OS and PFS. Gene mutations harboring prognostic impacts with uncorrected p-values < 0.05 are highlighted in Table 1 and Figure S10, and all survival analyses are presented in Table S7. We set an FDR threshold of 0.05 to detect gene mutations with significant prognostic impacts.

Among ABC DLBCL treated with R-CHOP, *TNFAIP3* mutations were significantly associated with lower OS ($FDR=7.86x10^{-4}$) and PFS ($FDR=3.04x10^{-2}$), while *GNA13* mutations were significantly associated with lower PFS ($FDR=3.04\ x10^{-2}$), (Figure 5). Of note, the poor prognostic impact of these mutations was not observed in patients treated with R-ACVBP, which, for *TNFAIP3* at least, might be linked to the improved survival observed in younger patients with DLBCL treated with R-ACVBP(48). These findings need to be confirmed in an independent cohort of patients, given the small sample size.

Unfortunately, the prognostic impact of *TNFAIP3* mutations in PMBL patients could not be assessed due to the existence of only one WT *TNFAIP3* PMBL patient treated with R-CHOP (Table S7). Moreover, previously described prognostic impacts of *TP53*, *FOXO1* or *MYD88*

mutations were not confirmed(35,49,50), although the impact of specific deleterious mutations was not analyzed on its own.

In conclusion, NGS is increasingly accessible in academic research settings, but its possibilities in routine clinical settings have yet to be thoroughly harnessed. This study has shown that, by using a restricted set of genes, not only can well-known mutations be tracked, but novel or rare mutations can also be identified and potentially targeted as well. Detailing subtype-enriched gene and pathway mutations is critical for optimal understanding and treatment of DLBCL: here, we have added to the field's current knowledge of the genetic heterogeneity between DLBCL subtypes, and identified novel clinical and prognostic correlations, which might also have an impact on therapeutic decisions. NGS with a consensus targeted panel could contribute valuable information to multidisciplinary meetings and constitute a molecular breakthrough in the way treatment decisions are made, by providing personalized mutational profiles of actionable targets. Furthermore, although this study was performed on frozen tumor samples, which are of limited availability, the Lymphopanel was designed to be effective in FFPE samples as well, further cementing its capacity to play an essential role in clinical disease management. In addition, our team has recently demonstrated that Lymphopanel NGS can be successfully performed using plasma-extracted cell-free circulating DNA, highlighting its feasibility and potential role in the monitoring of DLBCL(51). Taken together, these results serve as proof-of-principle that NGS with a consensus gene panel can alter the manner in which DLBCL patients are subclassified and treated.

Acknowledgements

This study was funded by grants from the Institut National du Cancer (INCA). We thank Marie-Hélène Delfau, Camille Laurent and Loïc Ysebaert for their critical review.

Contributors

SD, P-JV, SM, EB, PB, PR, J-PJ, MF, GS, HT, KL and FJ contributed to the conception and design of the study. TJM, FD, TF, CH, TL, CC-B, JB, TP, DC, BF, BC, RD, FP, AB, MA and NK collected clinical data. EB and CM performed NGS experiments. PP performed GEP experiments. SD, P-JV and SM performed statistical analyses and contributed to data interpretation. P-JV and SM developed the bioinformatics pipeline necessary for data

455 analysis. SD wrote the paper and all authors provided critical revisions and gave final
456 approval to submit for publication.

457

458 **Figure and Table Legends**

459 **Figure 1: Mutation frequencies in the total cohort and by subtype.** Mutation frequencies
460 in the total cohort are represented as a stacked bar chart. The number at the top of each bar
461 represents the mutation frequency of the indicated gene in the total cohort. Bars are
462 subdivided by DLBCL subtype, with segments proportional to mutation frequency.
463 Potentially actionable targets are highlighted by indicating the appropriate class of molecule,
464 which could potentially be used.

465 **Figure 2: Mutation pathway heterogeneity among DLBCL subtypes.** Pie-chart
466 representations of mutation frequencies represented by pathway are represented for ABC (A),
467 GCB (B), PMBL (C) and Other (D) subtypes. Mutation frequencies per gene and per subtype
468 are shown here as the percentage of the total number of variants. Genes were grouped into 8
469 specific pathways: Immunity (*CIITA*, *B2M*, *TNFRSF14* and *CD58*), NOTCH (*NOTCH1* and
470 *NOTCH2*), Apoptosis/Cell Cycle (*MFHAS1*, *XPO1*, *MYC*, *CDKN2A*/*B*, *FOXO1*, *TP53*,
471 *GNA13* and *BCL2*), NFkB (*TNFAIP3*, *MYD88*, *PIM1*, *CARD11*, *IRF4* and *PRDM1*),
472 Epigenetic Regulation (*EZH2*, *KMT2D*, *EP300*, *MEF2B* and *CREBBP*), MAP Kinases
473 (*BRAF*), JAK-STAT (*SOCS1* and *STAT6*), and BCR (*CD79A*/*B*, *ITPKB*, *TCF3* and *ID3*).

474 **Figure 3: Heatmap of mutation frequencies by subtype.** Mutation frequencies in each
475 subtype are indicated for each gene of the Lymphopanel. Mutation frequencies per gene and
476 per subtype are shown here as the percentage of the total number of patients. Statistical
477 significance of gene mutation enrichment in a given subtype is indicated by the FDR column.
478 The horizontal line separates genes with FDR<0.05, considered significant, from genes with
479 FDR≥0.05.

480 **Figure 4. Mutations at the protein level.** Protein representations were rendered using
481 domains imported from the Pfam database (green). Exons were located using the CCDS
482 database and were numbered automatically, not counting non-coding and spliced exons.
483 Substitutions are depicted as diamonds, insertions as triangles and deletions as rectangles
484 whose length varies according to the deletion size. A color code is also applied, with blue
485 indicating non-synonymous substitutions or non-frameshift insertions, yellow indicating
486 insertions and frameshift deletions, and pink indicating stop-gain and stop-loss mutations.
487 Blue shading indicates sequenced regions.

488 **Figure 5: *TNFAIP3* and *GNA13* mutations are linked to worse prognosis in R-CHOP-**
489 **treated ABC patients.** Survival analysis was performed on ABC patients treated with R-
490 CHOP according to the presence or absence of *TNFAIP3* mutation (A, B) or *GNA13* mutation
491 (C, D). Both *TNFAIP3* and *GNA13* mutations are associated with significantly less favorable
492 prognosis in R-CHOP treated ABC patients.

493 **Table 1. Prognostic impact of gene mutations among the Lymphopanel.** Gene mutations
494 with a tendency toward prognostic impact (uncorrected p<0.05) are indicated, for OS and/or
495 PFS. The subtype and treatment cohort in which a prognostic impact was identified is shown,
496 as is the number of mutant and WT patients for each survival analysis. HR column indicates
497 Hazard Ratio. Bold type highlights significant FDR values.

1. Swerdlow SH, Campo E, Harris NL, Jaffe ES, Pileri SA, Stein H, et al. WHO Classification of Tumours of Haematopoietic and Lymphoid Tissues. Lyon: IARC; 2008. 2008;

2. Alizadeh AAA, Eisen MBMB, Davis RE, Ma C, Lossos IS, Rosenwald A, et al. Distinct types of diffuse large B-cell lymphoma identified by gene expression profiling. Nature. 2000;403:503–11.

3. Wright G, Tan B, Rosenwald A, Hurt EH, Wiestner A, Staudt LM. A gene expression-based method to diagnose clinically distinct subgroups of diffuse large B cell lymphoma. Proceedings of the National Academy of Sciences of the United States of America. 2003;100:9991–6.

4. Huang JZ, Sanger WG, Greiner TC, Staudt LM, Weisenburger DD, Pickering DL, et al. The t(14;18) defines a unique subset of diffuse large B-cell lymphoma with a germinal center B-cell gene expression profile. Blood. 2002;99:2285–90.

5. Pfeifer M, Grau M, Lenze D, Wenzel S-S, Wolf A, Wollert-Wulf B, et al. PTEN loss defines a PI3K/AKT pathway-dependent germinal center subtype of diffuse large B-cell lymphoma. Proceedings of the National Academy of Sciences of the United States of America. 2013;110:12420–5.

6. Lenz G, Wright GW, Emre NCT, Kohlhammer H, Dave SS, Davis RE, et al. Molecular subtypes of diffuse large B-cell lymphoma arise by distinct genetic pathways. Proceedings of the National Academy of Sciences of the United States of America. 2008;105:13520–5.

7. Lenz G, Staudt LM. Aggressive lymphomas. The New England journal of medicine. 2010;362:1417–29.

8. Savage K, Monti S, Kutok J, Cattoretti G. The molecular signature of mediastinal large B-cell lymphoma differs from that of other diffuse large B-cell lymphomas and shares features with classical Hodgkin. Blood. 2003;102:3871–80.

9. Reichel J, Chadburn A, Rubinstein PG, Giulino-roth L, Tam W, Liu Y, et al. Flow sorting and exome sequencing reveal the oncogenome of primary Hodgkin and Reed-Sternberg cells. Blood. 2015;125:1061–73.

10. Salles G, de Jong D, Xie W, Rosenwald A, Chhanabhai M, Gaulard P, et al. Prognostic significance of immunohistochemical biomarkers in diffuse large B-cell lymphoma: a study from the Lunenburg Lymphoma Biomarker Consortium. Blood. 2011;117:7070–8.

11. Mareschal S, Ruminy P, Bagacean C, Marchand V, Cornic M, Jais J-P, et al. Accurate Classification of Germinal Center B-Cell-Like/Activated B-Cell-Like Diffuse Large B-Cell Lymphoma Using a Simple and Rapid Reverse Transcriptase-Multiplex Ligation-Dependent Probe Amplification Assay: A CALYM Study. The Journal of molecular diagnostics : JMD. 2015;

12. Scott DW, Mottok A, Ennishi D, Wright GW, Farinha P, Ben-Neriah S, et al. Prognostic Significance of Diffuse Large B-Cell Lymphoma Cell of Origin Determined by Digital Gene Expression in Formalin-Fixed Paraffin-Embedded Tissue Biopsies. Journal of clinical oncology : official journal of the American Society of Clinical Oncology. American Society of Clinical Oncology; 2015;33:2848–56.

13. Lohr JG, Stojanov P, Lawrence MS, Auclair D, Chapuy B, Sougnez C, et al. Discovery and prioritization of somatic mutations in diffuse large B-cell lymphoma (DLBCL) by whole-exome sequencing. Proceedings of the National Academy of Sciences of the United States of America. 2012;109:3879–84.

14. Morin RD, Mungall K, Pleasance E, Mungall AJ, Goya R, Huff RD, et al. Mutational and structural analysis of diffuse large B-cell lymphoma using whole-genome sequencing. Blood. 2013;122:1256–65.

15. Mullighan CG. Genome sequencing of lymphoid malignancies. Blood. American Society of Hematology; 2013;122:3899–907.

16. Morin RD, Johnson N a, Severson TM, Mungall AJ, An J, Goya R, et al. Somatic mutations altering EZH2 (Tyr641) in follicular and diffuse large B-cell lymphomas of germinal-center origin. Nature genetics. Nature Publishing Group; 2010;42:181–5.

17. Morin RD, Mendez-Lago M, Mungall AJ, Goya R, Mungall KL, Corbett RD, et al. Frequent mutation of histone-modifying genes in non-Hodgkin lymphoma. Nature. 2011;476:298–303.

18. Ngo VN, Young RM, Schmitz R, Jhavar S, Xiao W, Lim K-H, et al. Oncogenically active MYD88 mutations in human lymphoma. Nature. Nature Publishing Group; 2011;470:115–9.

19. Pasqualucci L, Trifonov V, Fabbri G, Ma J, Rossi D, Chiarenza A, et al. Analysis of the coding genome of diffuse large B-cell lymphoma. Nature genetics. Nature Publishing Group; 2011;43:830–7.

20. Zhang J, Grubor V. Genetic heterogeneity of diffuse large B-cell lymphoma. Proceedings of the National Academy of Sciences. 2013;110:1398–403.

21. Steidl C, Gascoyne RD. The molecular pathogenesis of primary mediastinal large B-cell lymphoma. Blood. 2011;118:2659–69.

22. Ritz O, Guiter C, Castellano F, Dorsch K, Melzner J, Jais J-P, et al. Recurrent mutations of the STAT6 DNA binding domain in primary mediastinal B-cell lymphoma. Blood. 2009;114:1236–42.

23. Khodabakhshi A, Morin R, Fejes A. Recurrent targets of aberrant somatic hypermutation in lymphoma. Oncotarget. 2012;3:1308–19.

24. Bohers E, Mareschal S, Bertrand P, Viailly PJ, Dubois S, Maingonnat C, et al. Activating somatic mutations in diffuse large B-cell lymphomas: lessons from next

generation sequencing and key elements in the precision medicine era. Leukemia & lymphoma. 2014;1–10.

25. Mareschal S, Dubois S, Viailly P-J, Bertrand P, Bohers E, Maingonnat C, et al. Whole exome sequencing of relapsed/refractory patients expands the repertoire of somatic mutations in diffuse large B-cell lymphoma. Genes, chromosomes & cancer. 2015;

26. Dubois S, Mareschal S, Picquenot J-M, Viailly P-J, Bohers E, Cornic M, et al. Immunohistochemical and genomic profiles of diffuse large B-cell lymphomas: Implications for targeted EZH2 inhibitor therapy? Oncotarget. 2015.

27. Foundation for Statistical Computing. R: A language and environment for statistical computing. Vienna, Austria;

28. Wilson WH, Young RM, Schmitz R, Yang Y, Pittaluga S, Wright G, et al. Targeting B cell receptor signaling with ibrutinib in diffuse large B cell lymphoma. Nature medicine. Nature Publishing Group; 2015;21:922–6.

29. Zheng X, Ding N, Song Y, Feng L, Zhu J. Different sensitivity of germinal center B cell-like diffuse large B cell lymphoma cells towards ibrutinib treatment. Cancer cell international. 2014;14:32.

30. Naylor TL, Tang H, Ratsch BA, Enns A, Loo A, Chen L, et al. Protein kinase C inhibitor sotrastaurin selectively inhibits the growth of CD79 mutant diffuse large B-cell lymphomas. Cancer research. 2011;71:2643–53.

31. Bohers E, Mareschal S, Bouzelfen A, Marchand V, Ruminy P, Maingonnat C, et al. Targetable activating mutations are very frequent in GCB and ABC diffuse large B-cell lymphoma. Genes, chromosomes & cancer. 2014;53:144–53.

32. Yang Y, Shaffer AL, Emre NCT, Ceribelli M, Zhang M, Wright G, et al. Exploiting synthetic lethality for the therapy of ABC diffuse large B cell lymphoma. Cancer cell. 2012;21:723–37.

33. Brault L, Menter T, Obermann EC, Knapp S, Thommen S, Schwaller J, et al. PIM kinases are progression markers and emerging therapeutic targets in diffuse large B-cell lymphoma. British journal of cancer. Nature Publishing Group; 2012;107:491–500.

34. Schuetz JM, Johnson N a, Morin RD, Scott DW, Tan K, Ben-Nierah S, et al. BCL2 mutations in diffuse large B-cell lymphoma. Leukemia. Nature Publishing Group; 2012;26:1383–90.

35. Xu-Monette ZY, Wu L, Visco C, Tai YC, Tzankov A, Liu W -m., et al. Mutational profile and prognostic significance of TP53 in diffuse large B-cell lymphoma patients treated with rituximab-CHOP: a report from an International DLBCL Rituximab-CHOP Consortium Program study. Blood. 2012;120:3986–97.

36. Schmitz R, Young RM, Ceribelli M, Jhavar S, Xiao W, Zhang M, et al. Burkitt lymphoma pathogenesis and therapeutic targets from structural and functional genomics. Nature. Nature Publishing Group; 2012;490:116–20.

611 37. Momose S, Weißbach S, Pischimarov J, Nedeva T, Bach E, Rudelius M, et al. The
612 diagnostic gray zone between Burkitt lymphoma and diffuse large B-cell lymphoma is
613 also a gray zone of the mutational spectrum. Leukemia. 2015;

614 38. Schmitz R, Hansmann M-L, Bohle V, Martin-Subero JI, Hartmann S, Mechtersheimer
615 G, et al. TNFAIP3 (A20) is a tumor suppressor gene in Hodgkin lymphoma and
616 primary mediastinal B cell lymphoma. The Journal of experimental medicine.
617 2009;206:981–9.

618 39. Weniger M a, Melzner I, Menz CK, Wegener S, Bucur a J, Dorsch K, et al. Mutations
619 of the tumor suppressor gene SOCS-1 in classical Hodgkin lymphoma are frequent and
620 associated with nuclear phospho-STAT5 accumulation. Oncogene. 2006;25:2679–84.

621 40. Ansell SM, Lesokhin AM, Borrello I, Halwani A, Scott EC, Gutierrez M, et al. PD-1
622 Blockade with Nivolumab in Relapsed or Refractory Hodgkin's Lymphoma. New
623 England Journal of Medicine. 2014;372:141206100011003.

624 41. Steidl C, Shah SP, Woolcock BW, Rui L, Kawahara M, Farinha P, et al. MHC class II
625 transactivator CIITA is a recurrent gene fusion partner in lymphoid cancers. Nature.
626 2011;471:377–81.

627 42. Maréchal Y, Pesesse X, Jia Y, Pouillon V, Pérez-Morga D, Daniel J, et al. Inositol 1, 3,
628 4, 5-tetrakisphosphate controls proapoptotic Bim gene expression and survival in B
629 cells. Proceedings of the National Academy of Sciences. 2007;104:13978–83.

630 43. Tagawa H, Karnan S, Kasugai Y, Tuzuki S, Suzuki R, Hosokawa Y, et al. MASL1, a
631 candidate oncogene found in amplification at 8p23.1, is translocated in immunoblastic
632 B-cell lymphoma cell line OCI-LY8. Oncogene. 2004;23:2576–81.

633 44. Jeromin S, Weissmann S, Haferlach C, Dicker F, Bayer K, Grossmann V, et al. SF3B1
634 mutations correlated to cytogenetics and mutations in NOTCH1, FBXW7, MYD88,
635 XPO1 and TP53 in 1160 untreated CLL patients. Leukemia. 2014;28:108–17.

636 45. Lapalombella R, Sun Q, Williams K, Tangeman L, Jha S, Zhong Y, et al. Selective
637 inhibitors of nuclear export show that CRM1/XPO1 is a target in chronic lymphocytic
638 leukemia. Blood. 2012;120:4621–34.

639 46. Mareschal S, Lanic H, Ruminy P, Bastard C, Tilly H, Jardin F. The proportion of
640 activated B-cell like subtype among de novo diffuse large B-cell lymphoma increases
641 with age. Haematologica. 2011;96:1888–90.

642 47. Dunleavy K, Pittaluga S, Maeda LS, Advani R, Chen CC, Hessler J, et al. Dose-
643 adjusted EPOCH-rituximab therapy in primary mediastinal B-cell lymphoma. The New
644 England journal of medicine. 2013;368:1408–16.

645 48. Récher C, Coiffier B, Haioun C, Molina TJ, Fermé C, Casasnovas O, et al. Intensified
646 chemotherapy with ACVBP plus rituximab versus standard CHOP plus rituximab for
647 the treatment of diffuse large B-cell lymphoma (LNH03-2B): an open-label
648 randomised phase 3 trial. Lancet (London, England). 2011;378:1858–67.

649 49. Trinh DL, Scott DW, Morin RD, Mendez-Lago M, An J, Jones SJM, et al. Analysis of
650 FOXO1 mutations in diffuse large B-cell lymphoma. Blood. 2013;121:3666–74.

651 50. Fernández-Rodríguez C, Bellosillo B, García-García M, Sánchez-González B, Gimeno
652 E, Vela MC, et al. MYD88 (L265P) mutation is an independent prognostic factor for
653 outcome in patients with diffuse large B-cell lymphoma. Leukemia. Nature Publishing
654 Group; 2014;28:2104–6.

655 51. Bohers E, Viailly P-J, Dubois S, Bertrand P, Maingonnat C, Mareschal S, et al.
656 Somatic mutations of cell-free circulating DNA detected by Next Generation
657 Sequencing reflect the genetic changes in both Germinal Center B-Cell like and
658 Activated B-Cell like Diffuse Large B-Cell Lymphoma tumors at the time of diagnosis.
659 Haematologica. Haematologica; 2015;haematol.2015.123612.

660

661

662

663

664

665

666

Author Manuscript Published OnlineFirst on January 27, 2016; DOI: 10.1158/1078-0432.CCR-15-2305
Author manuscripts have been peer reviewed and accepted for publication but have not yet been edited.

Gene	Subtype	Cohort	Type	Mutant (n)	WT (n)	HR	p	FDR
TNFAIP3	ABC	R-CHOP	OS	6	48	9.04 [2.82-28.98]	9.03E-06	**7.86E-04**
TNFAIP3	ABC	R-CHOP	PFS	6	48	5.59 [1.91-16.39]	4.29E-04	**3.04E-02**
GNA13	ABC	R-CHOP	PFS	5	49	5.89 [1.86-18.64]	6.47E-04	**3.04E-02**
B2M	all	R-CHOP	PFS	16	100	0.12 [0.03-0.55]	6.24E-03	3.25E-01
B2M	all	R-CHOP	OS	16	100	0.11 [0.01-0.82]	3.13E-02	5.43E-01
IRF4	all	R-CHOP	OS	10	106	2.53 [1.10-5.87]	2.98E-02	5.43E-01
CD79B	all	R-CHOP	OS	19	97	0.31 [0.11-0.90]	3.13E-02	5.43E-01
CD79B	all	R-CHOP	PFS	19	97	0.29 [0.10-0.83]	2.15E-02	5.58E-01
CD58	all	R-CHOP	PFS	12	104	2.36 [1.07-5.20]	3.27E-02	5.67E-01
GNA13	ABC	R-CHOP	OS	5	49	3.68 [1.21-11.15]	1.36E-02	5.94E-01
FOXO1	GC	R-CHOP	OS	5	35	3.87 [1.00-15.07]	3.53E-02	7.72E-01
CD79B	ABC	R-CHOP	OS	16	38	0.35 [0.12-1.02]	4.44E-02	7.72E-01
CD79B	ABC	R-CHOP	PFS	16	38	0.33 [0.11-0.95]	3.07E-02	8.30E-01

Table 1. Prognostic impacts of gene mutations among the Lymphopanel

Figure 1

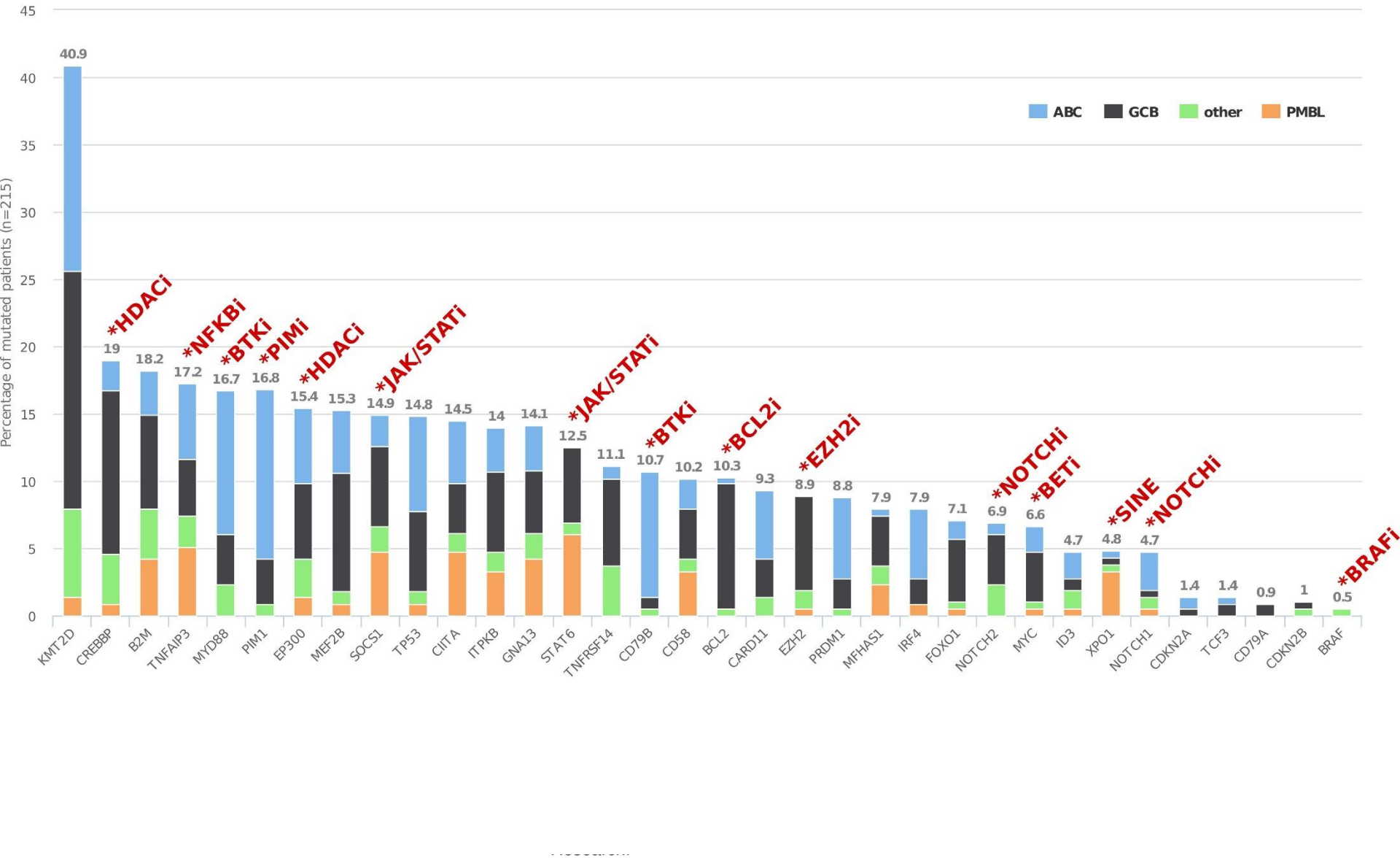
Percentage of mutated patients (n=215)
45
40
35
30
25
20
15
10
5
0
ABC
GCB
other
PMBL
40.9
19
18.2
17.2
16.7
16.8
15.4
15.3
14.9
14.8
14.5
14
14.1
12.5
11.1
10.7
10.2
10.3
9.3
8.9
8.8
7.9
7.9
7.1
6.9
6.6
4.7
4.8
4.7
1.4
1.4
0.9
1
0.5
*HDACi
*NFKBi
*BTKi
*PIMi
*HDACi
*JAK/STATi
*JAK/STATi
*BTKi
*BCL2i
*EZH2i
*NOTCHi
*BETi
*SINE
*NOTCHi
*BRAFi
KMT2D
CREBBP
B2M
TNFAIP3
MYD88
PIM1
EP300
MEF2B
SOCS1
TP53
CIITA
ITPKB
GNA13
STAT6
TNFRSF14
CD79B
CD58
BCL2
CARD11
EZH2
PRDM1
MFHAS1
IRF4
FOXO1
NOTCH2
MYC
ID3
XPO1
NOTCH1
CDKN2A
TCF3
CD79A
CDKN2B
BRAF

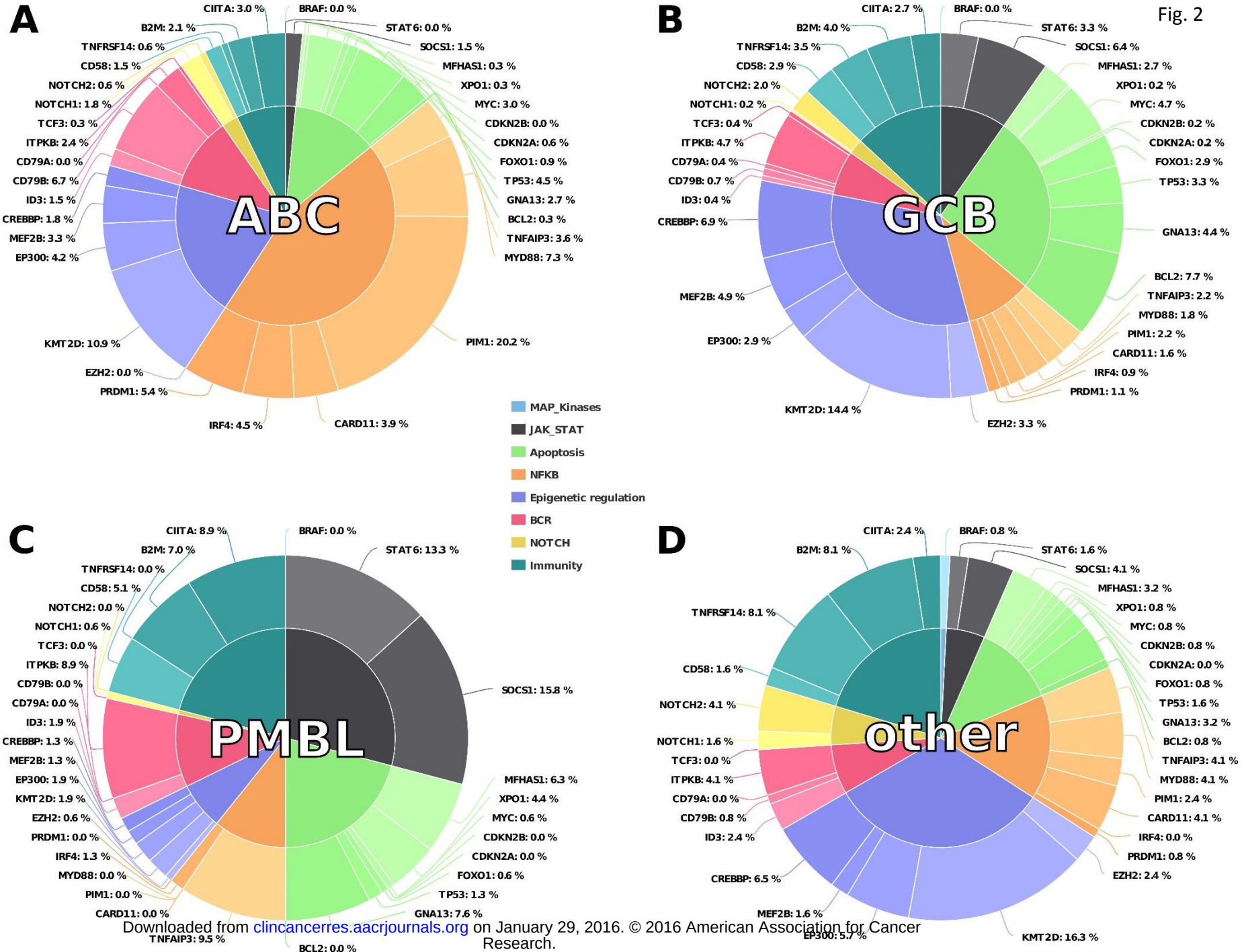

Figure 3

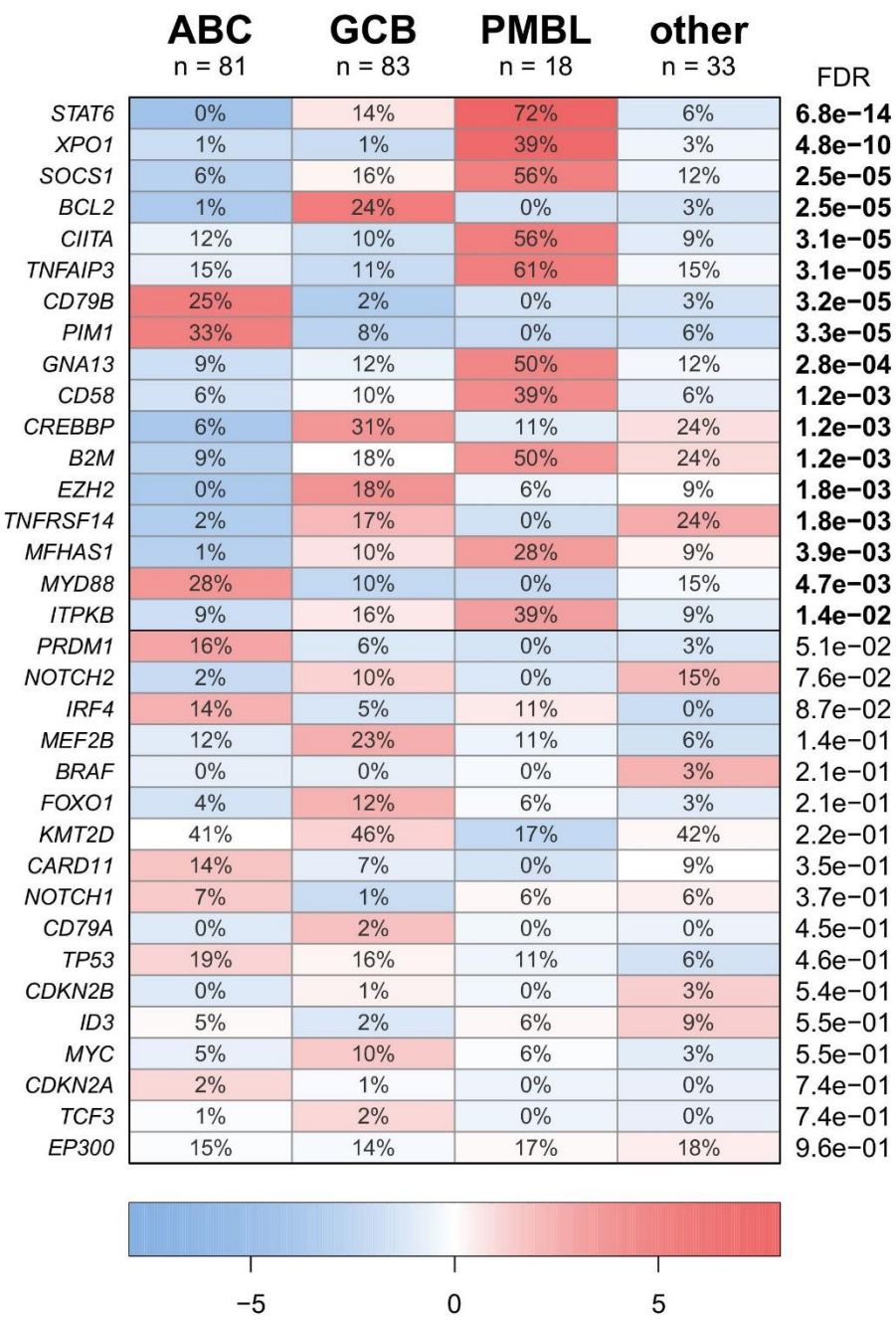

Figure 4

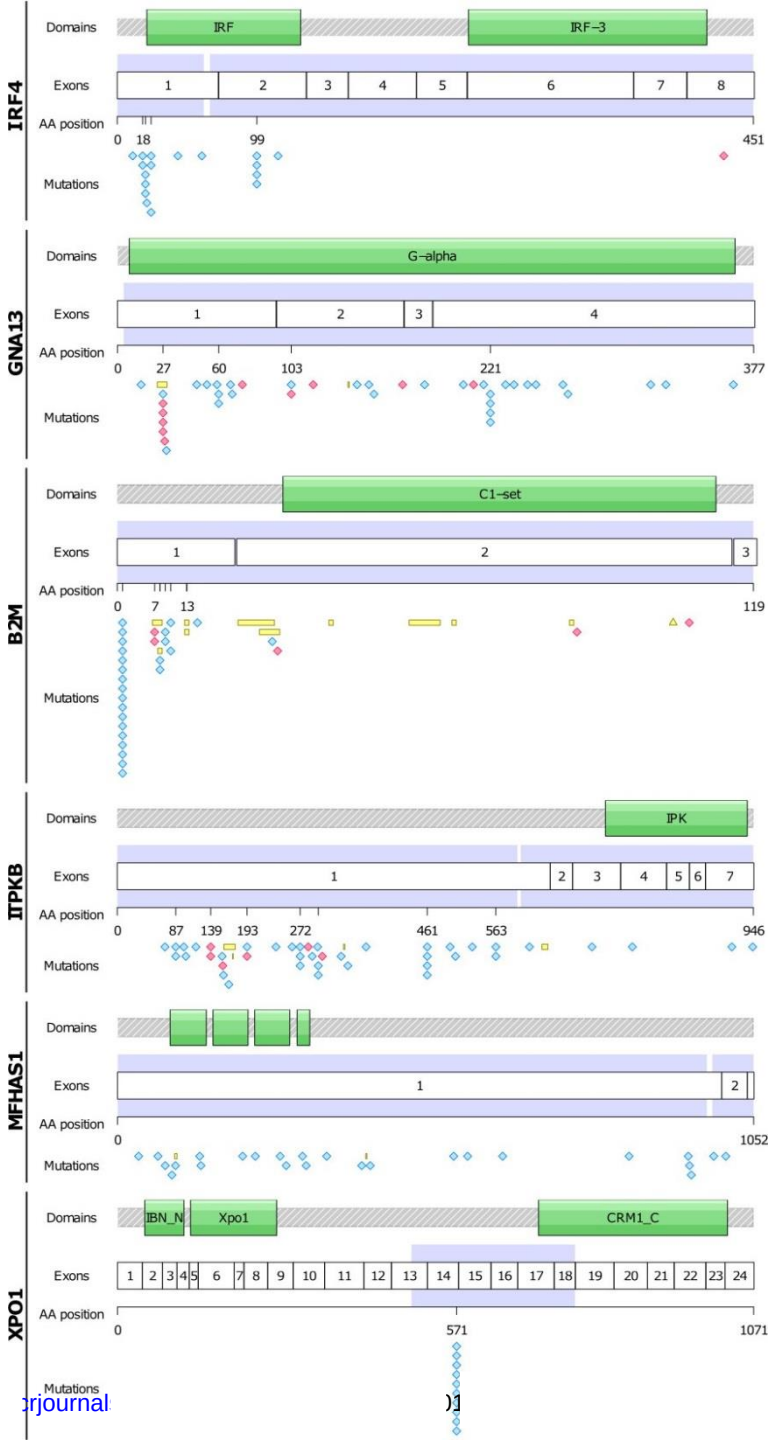
IRF4
Domains
IRF
IRF−3
Exons
1
2
3
4
5
6
7
8
AA position
0
18
99
451
Mutations
GNA13
Domains
G−alpha
Exons
1
2
3
4
AA position
0
27
60
103
221
377
Mutations
B2M
Domains
C1−set
Exons
1
2
3
AA position
0
7
13
119
Mutations
ITPKB
Domains
IPK
Exons
1
2
3
4
5
6
7
AA position
0
87
139
193
272
461
563
946
Mutations
MFHAS1
Domains
Exons
1
2
AA position
0
1052
Mutations
XPO1
Domains
IBN_N
Xpo1
CRM1_C
Exons
1
2
3
4
5
6
7
8
9
10
11
12
13
14
15
16
17
18
19
20
21
22
23
24
AA position
0
571
1071
Mutations

Figure 5

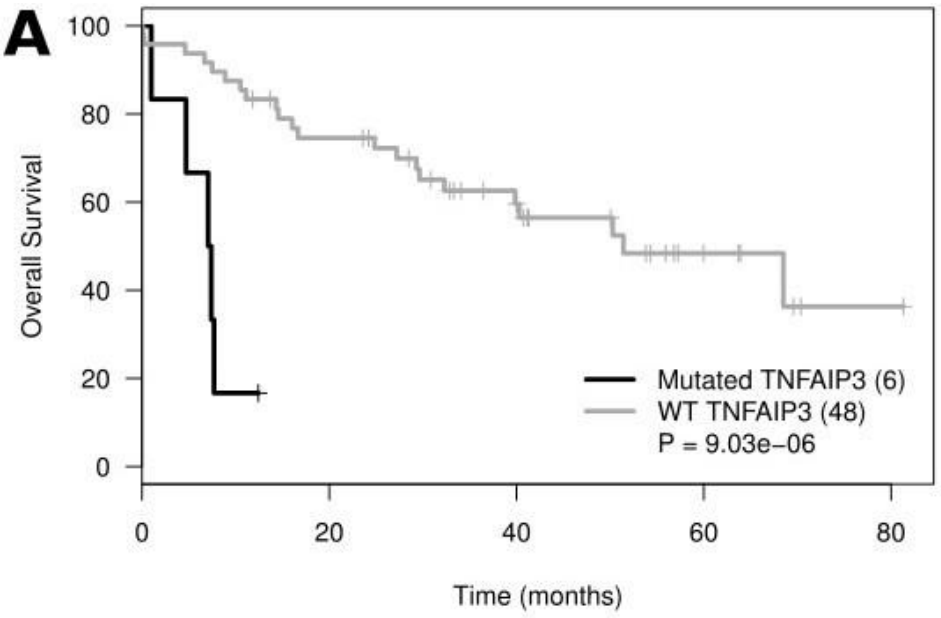
A
Overall Survival
100
80
60
40
20
0
0
20
40
60
80
Time (months)
Mutated TNFAIP3 (6)
WT TNFAIP3 (48)
P = 9.03e−06

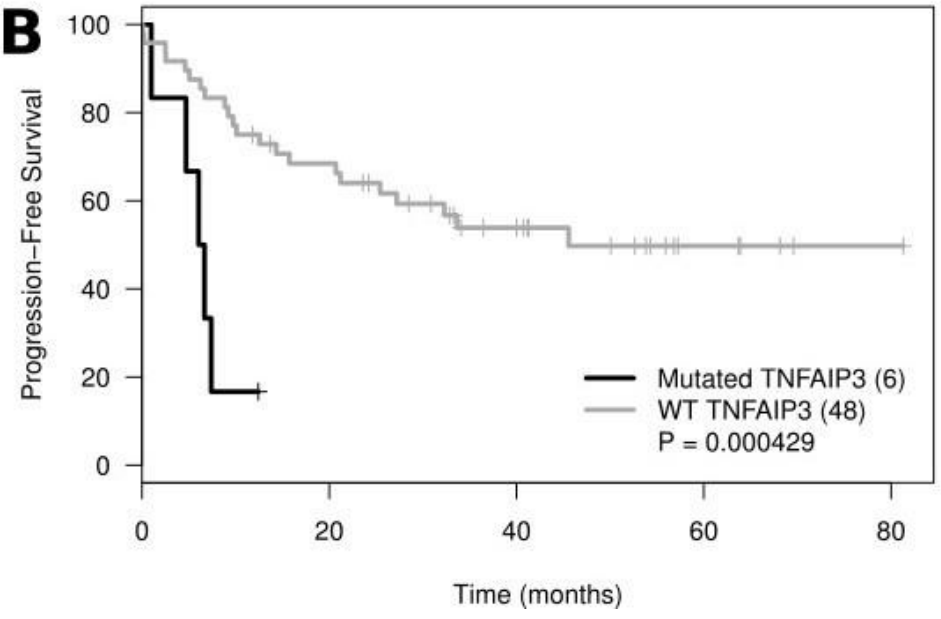
B
Progression−Free Survival
100
80
60
40
20
0
0
20
40
60
80
Time (months)
Mutated TNFAIP3 (6)
WT TNFAIP3 (48)
P = 0.000429

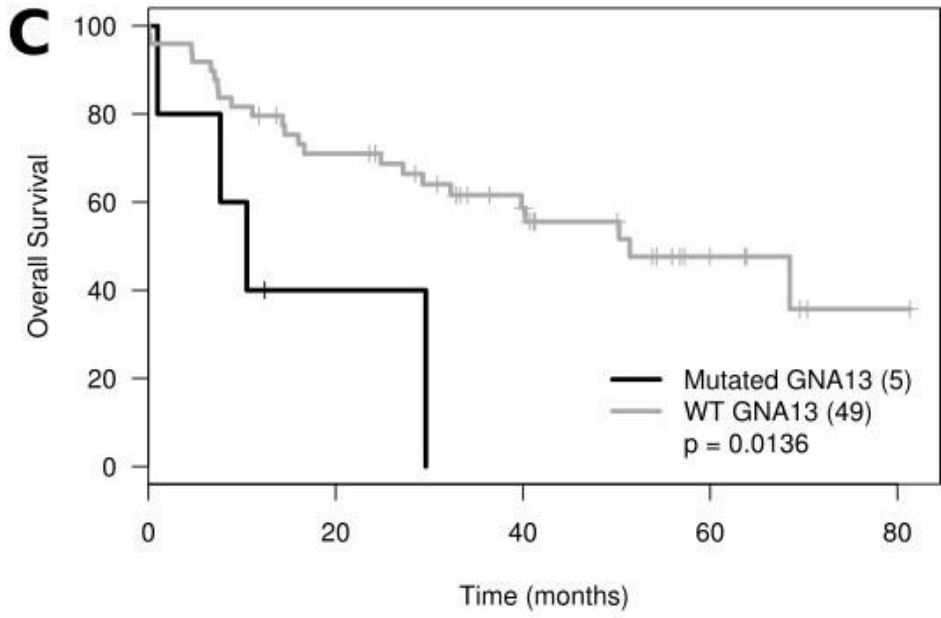
C
Overall Survival
100
80
60
40
20
0
0
20
40
60
80
Time (months)
Mutated GNA13 (5)
WT GNA13 (49)
p = 0.0136

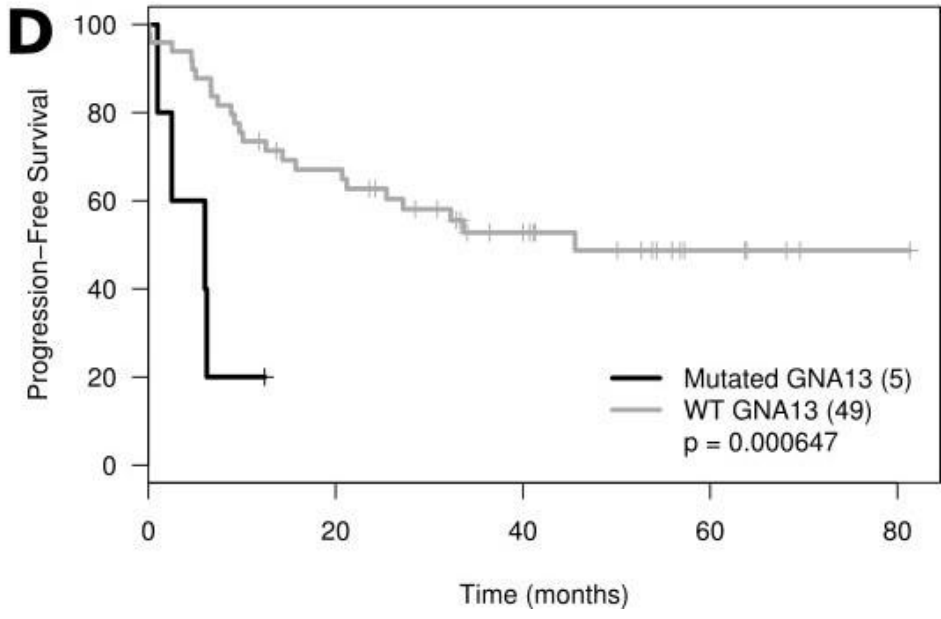
D
Progression−Free Survival
100
80
60
40
20
0
0
20
40
60
80
Time (months)
Mutated GNA13 (5)
WT GNA13 (49)
p = 0.000647